First operations with the new Collective Thomson Scattering diagnostic on the Frascati Tokamak Upgrade device

Bin, W.; Bruschi, A.; D'Arcangelo, O.; Castaldo, C.; Angeli, M. De; Figini, L.; Galperti, C.; Garavaglia, S.; Granucci, G.; Grosso, G.

Total number of authors:
21

Published in:
Journal of Instrumentation

Link to article, DOI:
10.1088/1748-0221/10/10/P10007

Publication date:
2015

Document Version
Publisher's PDF, also known as Version of record

First operations with the new Collective Thomson Scattering diagnostic on the Frascati Tokamak Upgrade device

2015 JINST 10 P10007

(http://iopscience.iop.org/1748-0221/10/10/P10007)

PUBLISHED BY IOP PUBLISHING FOR SISSA MEDIALAB

RECEIVED: *June 12, 2015*
REVISED: *July 17, 2015*
ACCEPTED: *July 30, 2015*
PUBLISHED: *October 8, 2015*

1st EPS CONFERENCE ON PLASMA DIAGNOSTICS (1STECPD)
14–17 APRIL 2015
FRASCATI, ROME, ITALY

First operations with the new Collective Thomson Scattering diagnostic on the Frascati Tokamak Upgrade device

W. Bin,[a,1] **A. Bruschi,**[a] **O. D'Arcangelo,**[b] **C. Castaldo,**[b] **M. De Angeli,**[a] **L. Figini,**[a] **C. Galperti,**[c] **S. Garavaglia,**[a] **G. Granucci,**[a] **G. Grosso,**[a] **S.B. Korsholm,**[d] **M. Lontano,**[a] **V. Mellera,**[a] **D. Minelli,**[a] **A. Moro,**[a] **A. Nardone,**[a] **S.K. Nielsen,**[d] **J. Rasmussen,**[d] **A. Simonetto,**[a] **M. Stejner**[d] **and U. Tartari**[a]

[a] *Istituto di Fisica del Plasma "P. Caldirola", Consiglio Nazionale delle Ricerche, via R. Cozzi 53, Milano, Italy*
[b] *ENEA for EUROfusion, Via E. Fermi 45, Frascati, Italy*
[c] *Centre de Recherches en Physique des Plasmas, Ecole Polytéchnique Fédérale de Lausanne, Route Cantonale, 1015 Lausanne, Switzerland*
[d] *Department of Physics, Technical University of Denmark, Anker Engelunds Vej 1 Bygning 101A, 2800 Kgs. Lyngby, Denmark*

E-mail: wbin@ifp.cnr.it

ABSTRACT: Anomalous emissions were found over the last few years in spectra of Collective Thomson Scattering (CTS) diagnostics in tokamak devices such as TEXTOR, ASDEX and FTU, in addition to real CTS signals. The signal frequency, down-shifted with respect to the probing one, suggested a possible origin in Parametric Decay Instability (PDI) processes correlated with the presence of magnetic islands and occurring for pumping wave power levels well below the threshold predicted by conventional models. A threshold below or close to the Electron Cyclotron Resonance Heating (ECRH) power levels could limit, under certain circumstances, the use of the ECRH in fusion devices. An accurate characterization of the conditions for the occurrence of this phenomenon and of its consequences is thus of primary importance. Exploiting the front-steering configuration available with the real-time launcher, the implementation of a new CTS setup now allows studying these anomalous emission phenomena in FTU under conditions of density and wave

[1] Corresponding author.

doi:10.1088/1748-0221/10/10/P10007

injection geometry that are more similar to those envisaged for CTS in ITER. The upgrades of the diagnostic are presented as well as a few preliminary spectra detected with the new system during the very first operations in 2014. The present work has been carried out under an EUROfusion Enabling Research project.

A shorter version of this contribution is due to be published in PoS at:
1st EPS conference on Plasma Diagnostics

KEYWORDS: Nuclear instruments and methods for hot plasma diagnostics; Microwave Antennas

Contents

1 Introduction

Since the first installation [1, 2] on the Frascati Tokamak Upgrade (FTU) device, the Collective Thomson Scattering (CTS) experiment was mostly devoted to the investigation of the thermal scattering of electron cyclotron waves in the propagation window below the 1st fundamental harmonic, hence in a condition similar to the one foreseen for the CTS diagnostic of fast ion distribution function in ITER. An additional and more recent aim of the experiment is to investigate the anomalous signals occasionally observed with the CTS diagnostics of different tokamaks, that may be correlated to the presence of rotating MHD magnetic islands.

Such signals were first observed in TEXTOR [3, 4], where a strong dependence of the measured power from the magnetic field and the plasma density was evidenced, as described in [4]. Similar evidences were subsequently found also in ASDEX and FTU. Recent theoretical models [5–7] attribute these anomalous emissions to a parametric decay instability (PDI) process occurring at a power threshold which is expected to be well below that predicted by more conventional models such as [8, 9], that instead foresee thresholds for PDI appearance largely exceeding the typical output power levels of gyrotrons. If confirmed, the occurrence of PDI phenomena might affect both the measurability of the CTS spectra, hence the use of CTS as a diagnostic for ions velocity distribution and, under some circumstances, the efficiency of ECRH in fusion devices. FTU offers the possibility to study the phenomenon in a plasma with electron density similar to that of ITER and a sub-harmonic millimeter wave probe can be injected in both ordinary and extraordinary propagation modes. The main aim of the CTS experiments in progress in FTU is to study the signal

2015 JINST 10 P10007

scattered from the position of the MHD tearing modes and to characterize the detected emissions as deeply as possible, exploiting a new system.

2 The new CTS diagnostic in FTU

2.1 Diagnostic layout

In the new CTS layout, the lower of the two lines of the real-time front-steering ECRH launcher of FTU [10–12] is used to launch the probe beam and the upper one to collect the signals. The launcher is shown in figure 1-left during laboratory tests at low power [13]. The upper line is designed either to inject ECH power or to collect radiation at 140 GHz for studies of reverse OXB mode coupling scheme [14, 15] or for the radiometric system during CTS experiments.

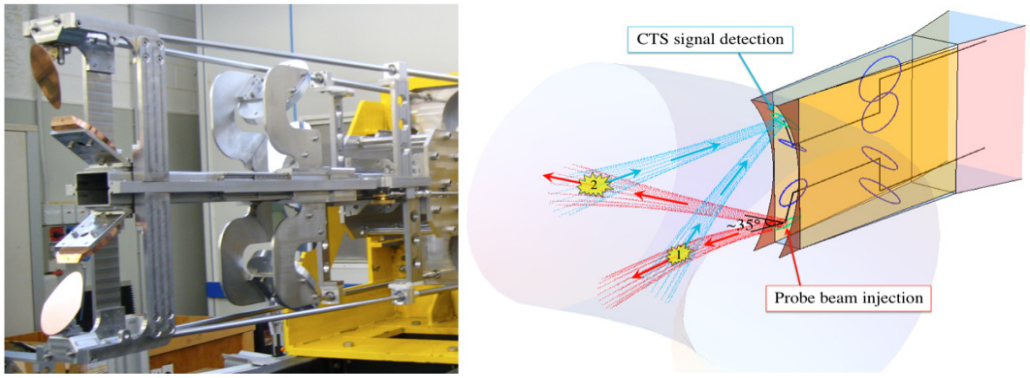

Figure 1. Left: picture of the two front steering electron cyclotron antennas used in new FTU CTS diagnostic to inject the probe beam (lower one) and to collect the scattering signal (upper one). Right: 3D view of the new CTS configuration from the vacuum vessel side. The CTS beams, simulated with beam tracing calculations, are shown while crossing at small toroidal angle ($\approx 0^\circ$) off-axis (intersection 1) and at wide toroidal angle ($\approx 35^\circ$) on-axis (intersection 2).

Two simulations of launched and received CTS beams are depicted in figure 1-right, showing, from the plasma side, the configuration of the two antennas of the front steering launcher, poloidally symmetric with respect to the equatorial plane. The simulation is made using GRAY [16], a quasi-optical beam tracing code that can compute electron cyclotron wave propagation, absorption and current drive in a general tokamak equilibrium.

The receiving line of the launcher [17, 18] is provided with a box for switching the collected radiation from the ECH transmission waveguide to the receiver front-end, connected to the 140 GHz radiometer. The transmission line used for delivering CTS signals from the torus hall to the radiometer has been recently installed on FTU. It consists of a mix of quasi-optical mirrors and a section of low loss HE_{11} overmoded corrugated waveguide with 88.9 mm diameter.

A pair of universal polarizers with $\lambda/4$ and $\lambda/8$ corrugation depths has been installed in front of the feed horn of the CTS receiver to match the (elliptically polarized) ordinary or extraordinary propagation mode to the linear polarization of the front-end. The control of the polarization of both injected and received beams opens the possibility to perform CTS experiments in FTU exploring all the possible combinations of propagation modes.

2015 JINST 10 P10007

A numerical code, developed on purpose, computes the polarization changes after the 20 reflections made in the CTS line, so allowing to define the correct configuration of the polarization section, which is checked also with low power measurements before starting the measurements.

2.2 Recent improvements in signal analysis

The CTS diagnostic of FTU has been recently improved with a new fast data acquisition, implemented for the first time in ASDEX [19], to allow studying the rapidly modulated emissions correlated with rotating islands. This system allows spectral reconstruction by direct FFT of the intermediate frequency signal and is added in parallel to the preexisting multi-channel spectrum analyzer, which was originally installed in FTU for thermal ion distribution measurements. The spectrum analyzer consists of a 32 channels filter bank optimized for double-sideband detection (where both sidebands are detected and overlapped into the same bandwidth) of 1.2 GHz around the local oscillator frequency, which is tuned at the same frequency as the probe beam (provided by a 140 GHz 500 kW GYCOM gyrotron).

The new digitizer (8 bit, NI PXIe-5186 express) is capable of resolving signals in an analog bandwidth of 5 GHz, with a maximum sampling rate of 12.5 GS/s and a maximum of two channels in parallel. The IF output from the radiometer front-end (which includes the local oscillator, the mixer and two cascaded amplifiers) is directly digitized and stored for off-line processing.

A dedicated software has been developed to Fourier transform the raw digital signals and to visualize the final spectra. Spectra are calibrated by acquiring the ECE signal in a shot where the fundamental resonance layer is in the plasma and no scattering phenomena or other kind of emissions occur. The broadband ECE emission of the plasma with a known temperature is nearly constant over the narrow detection band and can be taken as a reference. Data acquisition performed in parallel with both the digitizer (fast but with short time duration due to memory constraints) and the spectrum analyzer (whose signals are digitized at lower sampling rate for the whole shot duration) is of great help in case signals of different kind are simultaneously detected. The bandwidth of the digitizer is limited at present by the IF amplifiers installed after the mixer in the receiving chain and common to both systems. For this reason, the signal level decreases at intermediate frequencies beyond ~ 1.2 GHz, becoming undetectable at ~ 2.0 GHz. Since the mixer output band in principle can cover several GHz, an upgrade with more wideband amplifiers is scheduled. This will open the possibility to operate with the full 5 GHz digitizer bandwidth in the near future.

3 Starting operations with the new diagnostic

In the first experiments with the upgraded layout, started in 2014, signals were simultaneously collected from the fast digitizer and the spectrum analyzer during the plasma shots. A careful analysis of the antennas configuration was required to locate the scattering volume on the rational surfaces where the magnetic islands are located. This was carried out by simulating the propagation of the probing and the collected beams with the FTU plasma parameters. In FTU the magnetic islands, which may be either spontaneous (under certain plasma conditions) or induced by Neon or Argon injection, are typically located at the m:n=2:1 and m:n=3:2 rational surfaces

2015 JINST 10 P10007

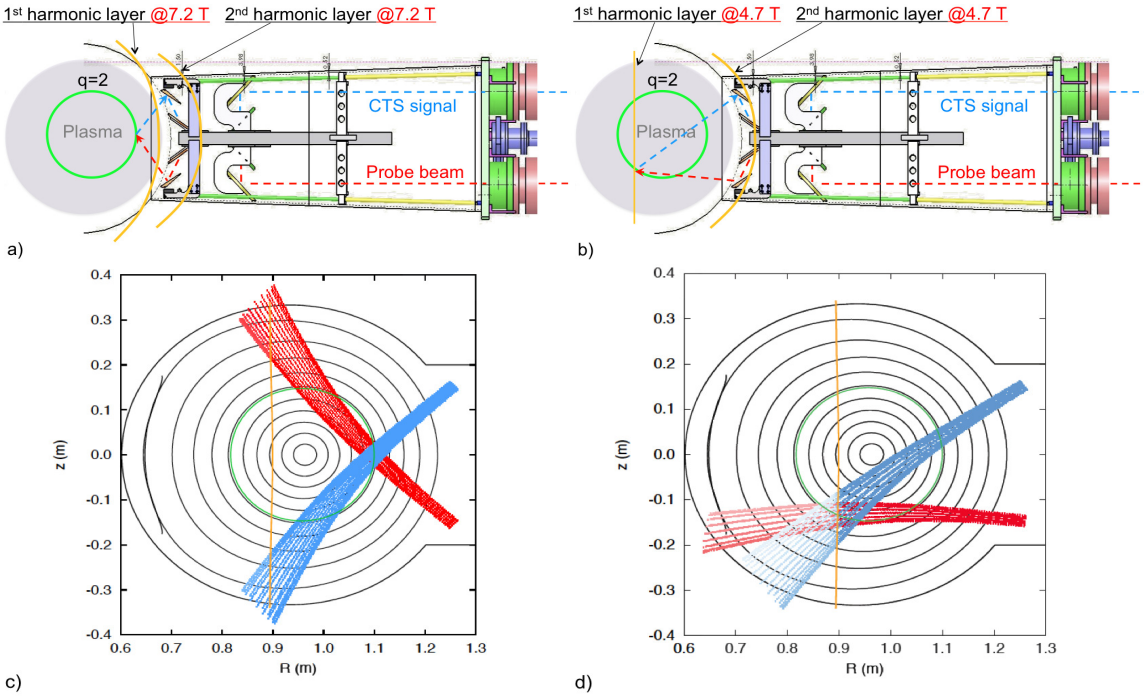

Figure 2. a: poloidal sketch of the FTU launcher where the probe beam (red) and the received beam (blue) are shown, intersecting on the equatorial plane at the plasma flux surface where the m:n=2:1 island forms. While the 1st and 2nd harmonic resonance layers are sketched for $B_T = 7.2\,T$, this configuration with intersection on the equatorial plane has been exploited also with $B_T = 4.7\,T$. b: configuration studied at $B_T = 4.7\,T$, where both the m:n=2:1 island and the 1st harmonic resonance layer are intersected by the scattering volume. In this case the two harmonic layers are sketched for $B_T = 4.7\,T$. Note that, in this case, the 2nd harmonic layer is closer to the backside of the mirrors with respect to the 7.2 T case. c, d: two beam tracing simulations taken from [20], both calculated for $B_T = 4.7\,T$ and with the antenna configurations a) and b) respectively, where the probe beam is in red, the receiving beam in light blue, the q= 2 surface in green and the resonant surface @5 T in orange.

3.1 High field scenario with $B_T = 7.2\,T$

Two plasma scenarios have been tested for the first time with the front steering launcher (see figure 2). The first one was with a toroidal field of B_T=7.2 T, such that the 1st electron cyclotron harmonic resonance (which for 140 GHz is @5 T) was out of the plasma on the low field side. Although in principle toroidal fields up to 8 T are available in FTU, B_T=7.2 T was chosen for sub-harmonic operation because at lower fields the fundamental resonance layer would shift too close to the plasma edge while at higher fields it would be very close to the antenna mirror, or even on it. The configuration with $B_T = 7.2\,T$ allows sub-harmonic CTS operations using a non-resonant probe whose frequency is below the fundamental harmonic in all the plasma volume and is the most similar to the one foreseen in the ITER CTS system. As in ITER, in the FTU sub-harmonic scenario the fundamental harmonic layer is located where the beam path is under vacuum. Nevertheless, it is worth noting that in FTU the 1st harmonic layer is always close to the vacuum vessel wall, in front of the plasma-facing mirror surfaces, even using a high toroidal field such as 7.2 T. On the other side, according to the present design of the CTS system [21, 22], the sub-harmonic operations

2015 JINST 10 P10007

in ITER are foreseen with the resonance layer far from the plasma edge. From the point of view of possible effects due to the beam passage at the resonance layer this may be different with respect to the FTU layout, since the risk of arcing depends on the local electric field and on the neutral gas density at the resonance location that will be more controllable in ITER than in FTU.

3.2 Low field scenario with $B_T = 4.7$ T

The second scenario was with a lower field of 4.7 T which leads to a positioning of the fundamental harmonic resonance in the plasma, on the high field side. The scenario with $B_T = 4.7$ T has been used for scattering measurements in two geometries. The former with the scattering volume in a region far from the resonant layer @5 T, by crossing the probe and the receiving beams in the low field side on the equatorial plane of the torus. The latter by intersecting the beams at the 1st harmonic resonance, with an asymmetric CTS configuration and the scattering volume out of the equatorial plane, in order to reach the m:n=2:1 island position at the same time. From the point of view of the launcher safety the main difference between the two scenarios consists in the position of the electron cyclotron harmonic layers (mainly the 1st harmonic layer in the 7.2 T scenario and 2nd harmonic layer in the 4.7 T case) with respect to the mirror used for the probe injection. In figures 2-a and 2-b a poloidal view of the FTU launcher is shown, where the two paths of the probe (red) and received (blue) beams are indicated, intersecting at the plasma flux surface where the m:n=2:1 island forms, on the equatorial plane in figure 2-a and out of it in figure 2-b. The 1st and 2nd harmonic resonance layers are sketched in figure 2-a for the case $B_T = 7.2$ T, the first one in front of the antenna mirrors (but outside the plasma), the second deeper in the port. This CTS configuration, with beams intersecting on the equatorial plane, has been exploited also in experiments where the toroidal magnetic field was 4.7 T. The CTS configuration in figure 2-b, was used instead only with $B_T = 4.7$ T. The two CTS beam intersect at the plasma flux surface where the m:n=2:1 island forms, but this time they also cross the 1st harmonic resonance layer. In figure 2-b the 1st and 2nd harmonic resonance layers are sketched for the case $B_T = 4.7$ T. It can be seen how only the 2nd harmonic layer is close to the launcher mirrors in this case. As can be noted in the beam tracing simulation shown in figure 2-c, the refraction in the plasma is such that, when operating with the configuration shown in figure 2-a, after the intersection with the receiving beam, a part of the probe wave impacts on the vacuum vessel wall and the rest passes through the resonance layer in a peripheral plasma region, where the density and the absorption efficiency should be very low. For this reason, part of the injected power is expected to reflect at the vessel walls and to diffuse in the camera using this configuration. The scenario with $B_T = 4.7$ T is more suitable for lowering such stray radiation and for absorbing the main beam, which turns out to be strongly dumped at the cyclotron harmonic layer. It is worth noting that the expected anomalous emissions due to PDIs should be considerably stronger than ECE. Therefore, in spite of a strong ECE which reduces the possibility to study the faint thermal CTS emissions, such a resonant scenario can be exploited to study possible PDIs phenomena.

3.3 Aims of the experiments

As a primary goal, the experiments being carried out in FTU are aimed at verifying the actual occurrence of the PDI phenomenon. In particular, the comparison between signals detected with the beam intersection shown in figure 2-a and 2-b in the 4.7 T scenario is expected to be helpful

2015 JINST 10 P10007

to verify whether the presence of possible anomalous emission is associated with any change of power absorption. The importance of verifying the actual occurrence of such effect lies in the fact that this may lead to a reduction of the ECRH efficiency, in particular when used as tool for neoclassical magnetic island control, which is at present the main scope of ECRH in ITER. The configuration shown in figure 2-b allows monitoring with CTS an injection scheme similar to the one used for tearing modes stabilization. To monitor the level of absorbed power during the shot time, the stray radiation level is measured using a system of 140 GHz sniffer probes [23] installed in the FTU vessel. A model has been developed to estimate, from the sniffer probes signals and from their angular positions in the camera with respect to the launching port, the absorption and the diffusion of the probe beam power. Also the comparison of resonant ($B_T = 4.7$ T) and non-resonant ($B_T = 7.2$ T) scenarios should be helpful to better comprehend possible interactions of PDIs on the ECH efficiency. The interception of the probe beam with the receiving line of sight has been studied for the two toroidal angles 5° and 35°. Angles lower than 5° are discarded to prevent possible direct back-reflections of power into the transmission line, while angles higher than 35° would be too close to the angular limits of the automatic protection system of the antenna steerable mirrors [24, 25]. The interest in studying CTS at different toroidal angles lies in the fact that when the angle between the magnetic field and the scattering vector (which is the difference between the two wave vectors of the incident and scattered radiation) approaches 90° modulations appear in the thermal CTS spectra at the ion cyclotron frequency ω_{ci} [26], while other emissions could be unaffected for any launching (and receiving) angle.

4 First experimental observations on the plasma

The FTU launcher allows a great flexibility and the capability to intersect the beams continuously over most of the plasma volume in real-time. Nevertheless, in the CTS experiments carried out up to now, the scattering volume has been located on the equatorial plane of the torus, whenever possible, to preserve the symmetry of the scattering configuration allowed by the two antennas, provided with two mirrors with an up-down symmetry in the poloidal plane with respect to the equatorial plane. A slight asymmetry of the configuration is inherently present in all discharges, due to the poloidal component of the magnetic field. Compared to the spatial resolution of the diagnostic [17], the inaccuracy induced by this asymmetry on the intersection of two beams launched and received with the same angles is small (of the order of 2 mm in both scenarios with $B_T = 4.7$ T and $B_T = 7.2$ T). Anyway, such small offset has been corrected during the experiments, by adjusting the angular steering of the mirrors according to the beam-tracing calculations.

The first operations at high toroidal field of 7.2 T were carried out without major technical problems. Such high field was expected to be the most critical for the safety of the launcher, due to the position of the injecting mirror close to the fundamental resonance layer, with a risk of mirror damage in case of plasma formation on the mirror surface by the injected beam. The safe operation of the probe beam injection at high field was confirmed both during experiments, by monitoring the plasma with UV spectroscopy for possible release of copper from the mirror, and at the end of the experiments, performing a visual inspection of the launcher frontend, which confirmed the good condition of the mirror after the operations with $B_T = 7.2$ T. The visual inspection has been carried out from the vacuum side of the vessel, using the inspection system described in [24].

2015 JINST 10 P10007

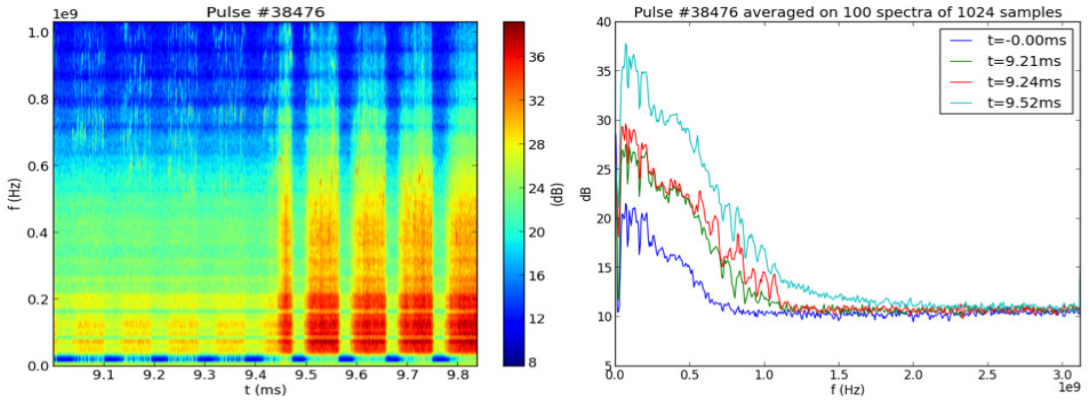

Figure 3. Left: uncalibrated spectra, displayed in dB, measured with the fast digitizer and with the intersection of the beams as in figure 2-a in shot #38476 ($B_T = 7.2$ T, with no relevant MHD activity detected by Mirnov coils). A transition from quiet to intense activity occurs at t$\approx$ 9.45. Time on abscissa starts from the end of an interval at the beginning of the pulse when the gyrotron frequency is unstable (leading the radiation frequency falling partially out of the notch filter cut-off frequency range) during which a pin diode blinds the receiver, in order to protect the mixer from the high level of stray radiation. A 10 kHz chopping (period of 0.1 ms) is also visible, made to exploit modulation-demodulation stages on the spectrum analyzer for increasing the signal-to-noise ratio. Frequencies in the spectra are measured in GHz (labeled as Hz, to be multiplied by the factor 10^9 indicated on top-left of the spectrogram). Right: a few spectra are shown at different times of the shot.

All measurements from the plasma have been carried out so far injecting and receiving ordinary polarized radiation. In the scattering spectra detected during the first experiments, different kinds of signals have been measured in the frequency range of 1.2 GHz from the probe frequency. The real origin of several signals (sometimes found with intensity level comparable to the core ECE emission, which typically in the CTS discharges is between 1 keV and 1.5 keV) is still under investigation and, at the present status, seems to be mostly ascribed to the gyrotron frequency instability found during the first phase of experiments, leading to exclude a real CTS nature.

The spectrum shown in figure 3 was acquired in shot #38476 ($B_T = 7.2$ T), with the scattering volume located where the q= 2 surface crosses the equatorial plane on the low field side of the torus, as in figure 2-a, and when no significant MHD activity was detected by Mirnov coils. In this shot, in a first phase of the gyrotron pulse, signals appear as broad lines at frequencies rapidly changing in time (visible only with the time resolution allowed by the digitizer) while, in a second phase, the power detected varies from quiet to more intense in a few tens of μs, with no apparent changes in the plasma conditions. Another example of spectrogram is shown in figure 4, this time measured at $B_T = 4.7$ T in shot #39005. Also this spectrogram has been acquired using the antenna configuration shown in figure 2-a. In this case the MHD activity, as monitored by Mirnov coils, seems to be completely absent. In this second spectrogram signals show emissions rapidly changing in time, in the form of bursts with spikes that repeat at high frequencies. Thermal CTS emission may be excluded in both the spectra shown in figure 3 and 4, since attenuation in this phase of experiments was too high to allow detection of such faint emissions. Anyway, in both the examples, the high resolution in time allowed by the new fast digitizer and the potential of the new diagnostic can be appreciated.

2015 JINST 10 P10007

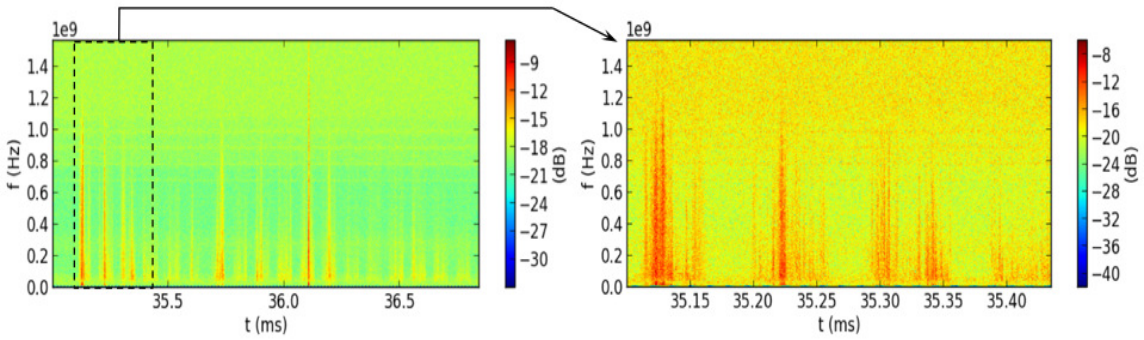

Figure 4. Left: another example of spectrogram measured @4.7 T with the fast digitizer acquisition and with the antenna configuration shown in figure 2-a. Despite no MHD activity is seen by magnetic probes rapid emissions are detected, in this case as bursts and spikes. Right: expanded view of dashed region on the left picture, showing the great time resolution available with the new fast digitizer. Also in these cases the overlapping modulation-demodulation stages made with 10 kHz chopping (period of 0.1 ms) is superimposed. Frequencies are measured in GHz (labeled as Hz, to be multiplied by the factor 10^9 indicated on top-left of both the spectrograms).

4.1 Investigation of breakdown plasma in the launching port

The formation of an undesired breakdown plasma in the port near the injecting mirror during probe beam injection is under investigation. In fact, while signals with a fast characteristic timescale, like those shown in figure 4, are still under investigation, breakdown in the port is the most plausible origin of the slow-timescale emission found in both the magnetic configurations at 4.7 T and at 7.2 T, likely due to backscattering of the gyrotron beam. An indication of breakdown in the antenna port is given by the appearance of gyrotron mode jumps in the cavity during the plasma discharges. Sometimes more than a single jump has been observed in the same shot, as in the case shown in figure 5-left, where broadband emission is detected (in shot #38995, $B_T = 4.7$ T) for most of the pulse length and two subsequent mode jumps occur before the gyrotron pulse stops. Strong signals appear in the spectrogram shown in figure 5-left, at well defined frequency interval from the probe after the second mode jump. The spectrogram has been acquired with the multi-channel spectrum analyzer.

This hypothesis is supported also by the strong light detected during several shots from the inner low field side of the FTU vacuum vessel using a visible light fast camera looking towards the ECRH launcher port. Figure 5-right shows a frame taken from a movie recorded with the camera during the ECRH injection in shot #38995, 90 ms after the beginning of the gyrotron pulse ($t_{gy} = 0.550$ s). The study and the characterization of this phenomenon may become important also in view of ITER, in particular in the proximity of the fundamental resonance in the sub-harmonic CTS scenario. The first aim is to investigate the conditions under which this phenomenon can be prevented. So far, no regulation of the toroidal magnetic field could be found to avoid breakdown in the port under all circumstances. The reason lies in the fact that the $\sim$ 1/R scaling of the iso-|B| layers no longer holds true outside the vessel and changes in B_T have a small effect on the position of the harmonic layer outside the vessel, which therefore is always in a region close to the last two mirrors, where beam convergence increases the local power density.

2015 JINST 10 P10007

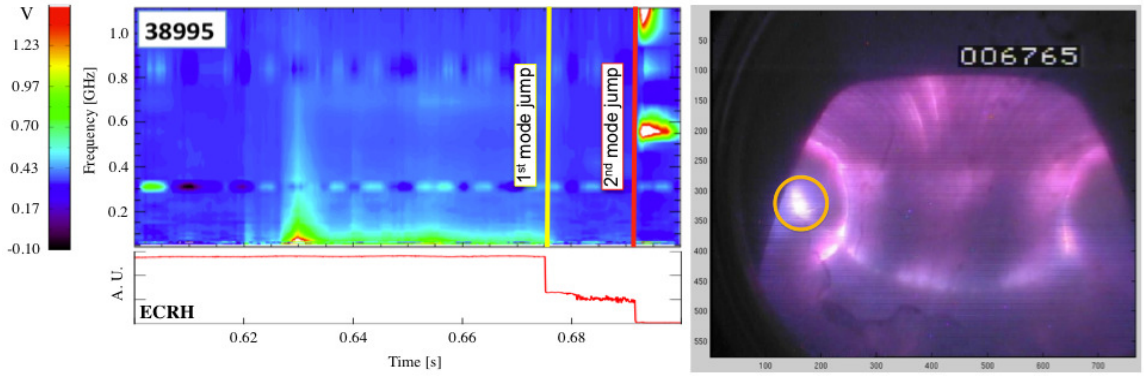

Figure 5. Left: broadband signals appearing in a spectrogram measured with the spectrum analyzer (shot #38995, units are V). The origin of this kind of emissions is ascribed to the formation of breakdown in the port. A first gyrotron mode jump (indicated with the yellow marker in the spectrogram) occurs at t≈0.675 s and can be seen (on bottom left, in arbitrary units) in the signal of the injected ECRH power in the transmission line measured by a directional coupler. This first mode jump is followed by a second jump (red marker in the spectrogram), after which two strong satellite gyrotron lines are detected with the receiver. Right: light detected during the pulse (at t= 0.640 s) from the inner low field side of the vacuum vessel (orange circle) with a visible light camera looking the ECRH port from 90° line of sight.

Three new sensors for detection of light and millimeter wave radiation have been installed during 2015 in the front-steering ECRH launcher port, in order to monitor breakdown as accurately as possible during the probe injection. The goal is to discriminate the signals due to local plasma generation from signals coming from the FTU plasma. The three systems have been installed on the vacuum flange of the two antennas used for CTS, and monitor the vacuum side of the launcher through two different optical windows. The sensors, which can be remotely controlled during the experiments, are shown in figure 6-left, as installed on the back flange of the launcher.

The first one is a visible-light CCD sensor camera (Toshiba®, model csu9001p, 12 mm diameter/12 mm focal length) installed on one of the two optical vacuum windows. The camera allows recording images from a line of sight looking to the inner side of the ECRH line used to inject the CTS probe. The evidence of breakdown in the antenna has been confirmed with the use of this camera. Light emission was detected during several ECRH pulses, and a similar light could be detected also with the visible camera looking at the launcher front from the vessel side (as in figure 5-right). A couple of images taken with this system are shown in figure 6-right. A frame taken during the discharge, when no power is injected, is shown on top of the figure (where only the light emitted by the plasma is detected from the vessel, on the far side), while a strong light emission due to breakdown in the port during the ECRH pulse is visible in the picture on the bottom.

The second sensor consists of an optical fiber (indicated with the green arrow in figure 6-left) formerly used in FTU for an electro-optical probe [27] and connected to a photon counter, acquiring signals from the same line of sight of the visible camera described above. The fiber shares the same support on the backside of the flange with the camera. This system has a time response much higher than the camera and acquires light data with a time resolution of 10 μs. The signals acquired with the fiber during the power injection confirmed the presence of strong emissions, in agreement with the other sensors. Both the visible camera and the optical fiber systems turn out to be reliable

2015 JINST 10 P10007

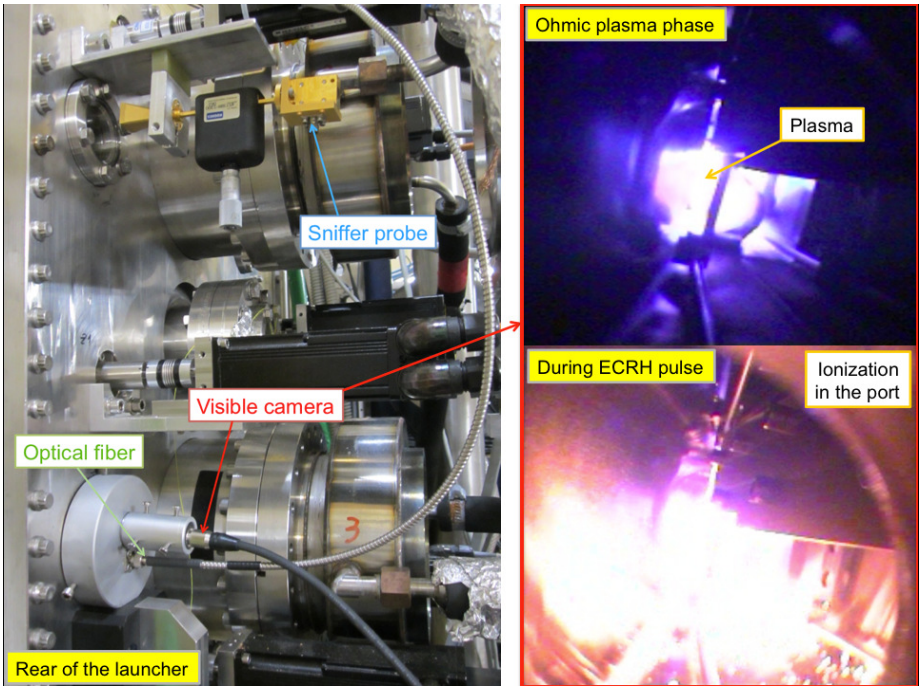

Figure 6. Left: picture of the vacuum flange on the backside of the FTU launcher. The visible camera, the optical fiber and the sniffer probe that have been recently installed to monitor breakdown in the port during the ECRH pulses are shown. The support of the visible camera and the optical fiber is the same and it is mounted on the external side of the vacuum window located on the lower part of the flange, while the sniffer probe is mounted alone in front of the second window, on the upper side of the flange. Right: two frames taken from a movie recorded with the visible camera in shot #39690 (@4.7 T). The first one is taken before the gyrotron pulse, showing light which comes only from the plasma and which is seen through the launcher. The second one is taken during EC injection, while breakdown is occurring in the launcher line.

diagnostics to monitor emissions from the port.

The third system, installed in front of the second optical vacuum window, is a sniffer probe that detects the level of stray radiation in the port. The sniffer is a Millitech DXP 08 detector whose signal can be directly acquired and stored in the FTU database and which now is automatically acquired during the plasma shots. This monitor (which has been already installed on the vessel port) is under commissioning at present, requiring proper signal conditioning and attenuation to operate during CTS experiments.

5 Future prospects

Apart from mode jumps ascribed to wave back-reflections from the port, sometimes the frequency stability of the gyrotron was not sufficient for accurate CTS measurements during the first experiments of 2014. Several frequency shifts arose during pulses, in a range up to some tens of MHz, with fast changes of about 0.5 GHz in around 50 μs, making the stray gyrotron radiation fall outside the notch filter central frequency. Experiments were performed with unusually large attenuation to protect the mixer from the stray power. In the beginning of 2015, an intervention on the high voltage power supply system of the gyrotron was made, with success, to improve frequency stability

2015 JINST 10 P10007

after the first strongly chirped phase (lasting tens of ms). The improved performance of the gyrotron was confirmed by measuring its frequency with both the fast digitizer and the multi-channel radiometer. A frequency measurement with the fast digitizer is shown in figure 7, where the local oscillator frequency (corresponding to 0 on the ordinates) was set about 90 MHz below the gyrotron frequency to allow a central visualization of the gyrotron line in the spectrogram.

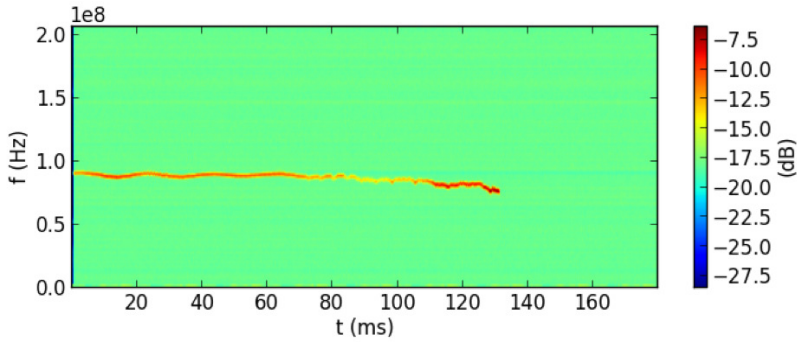

Figure 7. Gyrotron frequency measured with the fast digitizer after improvement of frequency stability. The signal was collected from the plasma, slightly detuning the gyrotron from the notch filter and setting front-end attenuation accordingly. Ordinates are labeled with Hz, to be multiplied by the factor 10^8 indicated on top-left.

A second radiometric system, to be used in parallel to the present one, is also being prepared for installation in the CTS diagnostic of FTU. The system is now in the laboratories at IFP-CNR (Milano) for off-line tests and refurbishment of front-end and back-end. Its installation in FTU is scheduled between the end of 2015 and the beginning of 2016. Both the front-end and the back-end of this system, that operated in the past in the W7-AS device [28], are very similar to those installed at present on FTU and now they have been reassembled.

The new radiometer is provided with 32 channels and a set of bandpass filters like the existing one. The overall system will be connected to a second branch of the CTS line and to the second channel of the fast digitizer. These upgrades will allow to perform measurements in FTU simultaneously with both channels of the fast digitizers (@6.25 GS/s of resolution each) and with both filter banks (32 channels each, acquired @2 kHz). The two synchronized radiometers will be used to detect radiation in both O- and X-mode at the same time, to identify emissions of different origin or, alternatively, to measure scattered signals from two different lines of sight. To this last aim, as already implemented in the ASDEX CTS system [29], a further receiving antenna and optics for matching it with the present receiving line are being designed also in FTU. The new receiving antenna will operate simultaneously to the current one and will be integrated in the same port and launcher used for CTS, between the injecting and receiving lines. The new system will allow a second line of sight for CTS experiments, with an angular capability of about $\pm 15^\circ$ in toroidal or poloidal direction, to be used also for cross-calibrations and reference of the background signal outside the magnetic island.

2015 JINST 10 P10007

6 Conclusions

The recent advances of the new CTS diagnostic installed on the FTU device consist in the addition of a new fast digitizer in parallel to the preexisting multi-channel spectrum analyzer and in the use of a new layout, exploiting the front steering ECRH launcher recently installed on FTU.

After a first characterization of the scattering configuration with beam tracing calculations, the first operation on the plasma started in 2014. Two different toroidal magnetic fields, 7.2 T and 4.7 T were used during the first experiments. Both scenarios have been explored for the first time with the front steering launcher of FTU. The two toroidal fields allowed to test two different regimes for CTS, the first one ($B_T = 7.2$ T) with a sub-harmonic probe beam, similar to the CTS configuration in ITER, and the second one ($B_T = 4.7$ T) with the fundamental electron cyclotron harmonic in the plasma. The first measurements on plasma in 2014 have been affected by a previously undetected frequency instability of the gyrotron, which forced to use high attenuation to protect the front-end from stray radiation falling outside the notch filter. Anyway, the spectra show several features that are presently under investigation.

The formation of a breakdown plasma in the antenna port during probe beam injection is the most likely origin of the emissions on a slow timescale and of spectral lines associated with gyrotron mode jumps found during the operations.

Three new sensors have been installed on the CTS antenna system: a camera and an optical fiber to detect visible light emission in the launching antenna port, and a sniffer probe detector, to measure the 140 GHz stray radiation at the probe injection point. The three sensors will help in the discrimination of signals originating in the port from those coming from the plasma.

In 2015, the gyrotron used for the probe beam has been stabilized in frequency. Now the CTS gyrotron is ready to be used for the new upcoming experiments.

Finally, a second radiometric system is also being prepared for measurements using both channels of the fast digitizers and two filter banks and radiometers. This will open the possibility to measure scattered radiation in O-mode and X-mode simultaneously and to receive signals from two different lines of sight in the plasma using a new receiving antenna.

Acknowledgments

This work has been carried out within the framework of the EUROfusion Consortium and has received funding from the Euratom research and training programme 2014-2018 under grant agreement No 633053. The views and opinions expressed herein do not necessarily reflect those of the European Commission.

References

[1] F. Orsitto et al., *Characterization and preliminary results of the collective Thomson scattering system on FTU tokamak*, *Rev. Sci. Instrum.* **70** 1 (1999) 1158.

[2] U. Tartari et al., *Evolution of the millimeter-wave collective Thomson scattering system of the high-field tokamak Frascati Tokamak Upgrade*, *Rev. Sci. Instrum.* **78** (2007) 043506.

[3] E. Westerhof et al., *Strong Scattering of High Power Millimeter Waves in Tokamak Plasmas with Tearing Modes*, *Phys. Rev. Lett.* **103** (2009) 125001.

2015 JINST 10 P10007

[4] S.K. Nielsen et al., *Experimental characterization of anomalous strong scattering of mm-waves in TEXTOR plasmas with rotating islands*, *Plasma Phys. Control. Fusion* **55** (2013) 115003.

[5] A.Y. Popov and E.Z. Gusakov, *Low-threshold absolute two-plasmon decay instability in the second harmonic electron cyclotron resonance heating experiments in toroidal devices*, *Plasma Phys. Control. Fusion* **57** (2015) 025022.

[6] E.Z. Gusakov and A.Y. Popov, *On the possibility of low-threshold anomalous absorption in tokamak 2nd-harmonic electron cyclotron resonance heating experiments*, *Europhys. Lett.* **99** (2012) 15001.

[7] A.Y. Popov, E.Z. Gusakov and A.N. Saveliev, *On the low-threshold parametric mechanism of the anomalous power absorption in electron cyclotron resonance heating experiments in toroidal devices*, *JETP Lett.* **96** (2012) 164.

[8] A.G. Litvak et al., *On nonlinear effects in electron-cyclotron resonance plasma heating by microwave radiation*, *Phys. Fluids B* **5** (1993) 4347.

[9] M. Porkolab and B.I. Cohen, *Parametric instabilities associated with intense electron cyclotron heating in the MTX tokamak*, *Nucl. Fusion* **28** (1988) 239.

[10] W. Bin et al., *Design of a new ECRH launcher for FTU tokamak*, *Fusion Eng. Des.* **84** (2009) 451.

[11] A. Bruschi et al., *A new launcher for real-time ECRH experiments on FTU*, *Fusion Sci. Technol.* **55** (2009) 94.

[12] S. Garavaglia et al., *Installation, integration and power tests of the new fast ECRH launcher of FTU*, *Fusion Eng. Des.* **88** (2013) 998.

[13] A. Moro et al., *Low power tests on the new front steering EC launcher for FTU*, *Fusion Eng. Des.* **86** (2011) 942.

[14] W. Bin et al., *Feasibility study of O-X coupling for overdense plasma heating through O-X-B mode conversion in FTU*, *Nucl. Fusion* **53** (2013) 083020.

[15] W. Bin et al., *A real-time tracking for optimal wave injection in overdense plasma heating experiments at 140 GHz in FTU*, *IEEE Trans. Plasma Sci.* **40** (2012) 622.

[16] D. Farina, *A quasi-optical beam-tracing code for electron cyclotron absorption and current drive: GRAY*, *Fusion Sci. Technol.* **52** (2007) 154.

[17] W. Bin et al., *The upgraded Collective Thomson Scattering diagnostics of FTU*, *Fusion Eng. Des.* **96-97** (2015) 733.

[18] A. Bruschi et al., *The upgraded Collective Thomson Scattering diagnostic of FTU for ion temperature and PDI investigations*, in 9^{th} *International Workshop Strong Microwaves and Terahertz Waves: Sources and Applications* (2014).

[19] M. Stejner et al., *Resolving the bulk ion region of millimeter-wave collective Thomson scattering spectra at ASDEX Upgrade*, *Rev. Sci. Instrum.* **85** (2014) 093504.

[20] A. Bruschi et al., *Experimental studies with the improved CTS diagnostics on FTU and evidences of scattered wave signals with short time-scale*, in *Proceedings of the* 42^{nd} *European Physical Society Conference on Plasma Physics* (2015).

[21] F. Leipold et al., *Antenna design for fast ion collective Thomson scattering diagnostic for the international thermonuclear experimental reactor*, *Rev. Sci. Instrum.* **80** (2009) 093501.

[22] F. Meo et al., *Design of the collective Thomson scattering diagnostic for International Thermonuclear Experimental Reactor at the 60 GHz frequency range*, *Rev. Sci. Instrum.* **75** (2004) 3585.

2015 JINST 10 P10007

[23] F. Gandini et al., *The detection of the non-absorbed millimeterwave power during EC heating and current drive*, *Fusion Eng. Des.* **56-57** (2001) 975.

[24] W. Bin et al., *Antenna system analysis and design for automatic detection and real-time tracking of electron Bernstein waves in FTU*, 2014 *JINST* **9** P05001.

[25] R. Ferrero et al., *Dynamic tests on the new front-steering ECH&CD launcher for FTU*, *Fusion Eng. Des.* **86** (2011) 1009.

[26] S.B. Korsholm et al., *Measurements of Intrinsic Ion Bernstein Waves in a Tokamak by Collective Thomson Scattering*, *Phys. Rev. Lett.* **106** (2011) 165004.

[27] De Angeli et al., *Note: Simultaneous electrical and optical detection of expanding dense partially ionized vapour clouds*, *Rev. Sci. Instrum.* **82** (2011) 106101.

[28] E.V. Suvorov et al., *Collective Thomson scattering at W7-AS*, *Plasma Phys. Control. Fusion* **39** (1997) B337.

[29] S.K. Nielsen et al., *Measurements of the fast-ion distribution function at ASDEX upgrade by collective Thomson scattering (CTS) using active and passive views*, *Plasma Phys. Control. Fusion* **57** (2015) 035009.

2015 JINST 10 P10007